0090-9556/10/3810-1731–1739$20.00
DRUG METABOLISM AND DISPOSITION
Vol. 38, No. 10
33845/3627051
Printed in U.S.A.
Copyright © 2010 by The American Society for Pharmacology and Experimental Therapeutics
DMD 38:1731–1739, 2010

DMD

DRUG METABOLISM AND DISPOSITION

aspet

Microsomal Cytochrome P450-Mediated Metabolism of Protopanaxatriol Ginsenosides: Metabolite Profile, Reaction Phenotyping, and Structure-Metabolism Relationship

Haiping Hao, Li Lai, Chaonan Zheng, Qiong Wang, Guo Yu, Xueyan Zhou, Liang Wu, Ping Gong, and Guangji Wang

Key Laboratory of Drug Metabolism and Pharmacokinetics, Key Unit of State Administration of Traditional Chinese Medicine for Pharmacokinetic Methodology of Traditional Chinese Medicine Complex Prescription, China Pharmaceutical University, Nanjing, China (H.H., L.L., C.Z., Q.W., G.Y., X.Z., L.W., P.G., G.W.); and National Chengdu Center for Safety Evaluation of Drugs, West China Hospital, Sichuan University, Chengdu, China (L.L.)

Received April 6, 2010; accepted July 16, 2010

ABSTRACT:

Although the biotransformation of ginsenosides in the gastrointestinal tract has been extensively studied, much less is known about hepatic cytochrome P450 (P450)-catalyzed metabolism. The major aims of this study were to clarify the metabolic pathway and P450 isoforms involved and to explore the structure-metabolism relationship of protopanaxatriol (PPT)-type ginsenosides in hepatic microsomes. Efficient depletion of ginsenoside Rh1, Rg2, Rf, and PPT was found, whereas the elimination of Re and Rg1, characterized by a glucose substitution at the C20 hydroxy group, was negligible in microsomal incubation systems. Based on high-performance liquid chromatography hybrid ion trap and time-of-flight mass spectrometry analysis, the oxygenation metabolism on the C20 aliphatic branch chain was identified as the predominant metabolic pathway of PPT ginsenosides in both human and rat hepatic microsomes. By a comparison with authentic standards, the C24–25 double bond was identified as one of the oxygenation sites to produce the metabolites of C20–24 epoxide (ocotillol-type ginsenosides). Both chemical inhibition and human recombinant P450 isoform assays indicated that CYP3A4 was the predominant isozyme responsible for the oxygenation metabolism of PPT ginsenosides. Enzyme kinetic evaluations in rat and human hepatic microsomes and human recombinant CYP3A4 isozyme incubation systems showed generally consistent results in that the intrinsic clearance ranked as Rf ≤ Rg2 < Rh1 < PPT, closely correlating with logP values and the number of glycosyl substitutions. Results obtained from this study suggest that CYP3A4-catalyzed oxygenation metabolism plays an important role in the hepatic disposition of ginsenosides and that glycosyl substitution, especially at the C20 hydroxy group, determines their intrinsic clearances by CYP3A4.

Introduction

Ginseng has been one of the most popular herbal medicines used in Oriental counties (*Panax ginseng* C.A. Meyer, Asian ginseng) to treat many diseases over 2000 years and also became known in the West (*Panax quinquefolius* L., American ginseng) by the 18th century (Gillis, 1997; Attele et al., 1999). More than 100 kinds of protopanaxadiol (PPD)- and protopanaxatriol (PPT)-type ginsenosides have been identified and claimed to be responsible for the wide therapeutic effects of ginseng and its various preparations (Christensen, 2009). A large number of references are available in the current body of literature, contributing to the pharmacological activities, underlying mechanisms, pharmacokinetic behaviors, and biotransformation of ginsenosides (Jia et al., 2009; Jia and Zhao, 2009). One of the important findings is that both PPD- and PPT-type ginsenosides always undergo sequential deglycosylation metabolism catalyzed by gastric acid and intestinal bacteria in biological conditions to form secondary metabolites and finally aglycones with enhancing biological activities and better pharmacokinetic characteristics (Liu et al., 2009). For example, ginsenoside Rg3 sequentially degraded in rat gastrointestinal tract to Rh2 and PPD, both of which were absorbed into the circulation system and characterized with higher plasma exposure levels (Xie et al., 2005) and stronger antitumor activities than ginsenoside Rg3 itself (Bae et al., 2004). Such important findings strongly indicate that the biotransformation and metabolic

This work was supported by the Natural Science Foundation of Jiangsu province [Grants BK2007169, BK2008038]; the Foundation for the Author of National Excellent Doctoral Dissertation of the People's Republic of China [Grant 200979]; the National Natural Science Foundation of the People's Republic of China [Grants 30630076, 30801422]; and the National Key New Drug Creation Special Programme [Grants 2009ZX09304-001, 2009ZX09502-004].

H.H. and L.L. contributed equally to this work.

Article, publication date, and citation information can be found at http://dmd.aspetjournals.org.

doi:10.1124/dmd.110.033845.

ABBREVIATIONS: PPD, protopanaxadiol; PPT, protopanaxatriol; P450, cytochrome P450; LC/MS-IT-TOF, high-performance liquid chromatography hybrid ion trap and time-of-flight mass spectrometry; Ket, ketoconazole; Naph, α-naphthoflavone; Sul, sulfaphenazole; Qui, quinidine; DDC, diethyl dithiocarbamate; TP, ticlopidine hydrochloride; Orph, orphenadrine citrate salt; 6-P-G, glucose 6-phosphate; PDH, glucose-6-phosphate dehydrogenase.

Downloaded from dmd.aspetjournals.org at Beijing Book Co Inc/PeriodicalsZhejiang Med Univ Lib/783081 on May 2, 2013

DMD DRUG METABOLISM AND DISPOSITION aspet

studies are of great significance in disclosing the therapeutic mysteries of ginsenosides.

Despite intensive research on ginsenoside biotransformation in previous decades, most of these studies are largely limited to the sugar cleavage reactions catalyzed by gastric acid and/or intestinal bacteria. To date, little is known about the further metabolic fate of such ginsenosides and their degradation products absorbed into the circulation system, where hepatic microsomal drug-metabolizing enzymes play an important role in disposition of many synthesized drugs and natural products. We have recently identified two monooxygenated metabolites from bile and urine samples of rats treated intravenously with ginsenoside Rh1 and also from in vitro hepatic microsomal incubation media (Lai et al., 2009a). Oxygenated metabolites had been also identified for Rg3 (Qian et al., 2005b), Rh2 (Qian et al., 2005a), and Rd (Yang et al., 2007) in rats and for PPT in rat hepatic microsomes (Kasai et al., 2000). Moreover, some previous reports demonstrated that various ginsenosides and especially their degradation products were capable of modulating cytochrome P450 enzyme activities (Liu et al., 2006a,b; Etheridge et al., 2007; Wang et al., 2008). Such evidence strongly suggests that the microsomal cytochrome P450 enzymes may play an important role in the systematic disposition of ginsenosides that finally reach the systemic circulation after oral ingestion. Because intact ginsenosides and their degradation products reaching the circulation system are of therapeutic benefit in most cases, the detailed hepatic microsomal-mediated metabolism of ginsenosides proposed in this study will be of great significance for better understanding of their systematic disposition and of ginseng-drug interaction and the mechanisms involved.

The present study was designed to be a comprehensive study on the microsomal-mediated metabolism of PPT-type ginsenosides. Five major PPT-type ginsenosides including 20(*S*)-ginsenoside Re, Rg1, Rg2, Rf, and Rh1 and the aglycone PPT (Fig. 1) were included in this study to evaluate the microsomal-mediated metabolism, including metabolic profiling in both human and rat microsomal incubation systems through LC/MS-IT-TOF analysis, reaction phenotyping using human recombinant P450 isoforms and specific chemical inhibitors, and structure-metabolism relationship assessment based on enzyme kinetics analysis. The components were selected in consideration of their high contents in various ginseng preparations, well proven pharmacological activities, and coverage of structural characteristics of PPT-type ginsenosides (attached with zero to three glycosyl groups).

Materials and Methods

Chemicals and Reagents. Ginsenoside Re, Rg1, Rg2, Rf, Rh1, pseudo-ginsenoside RF11 and RT5, and PPT (purity >98%) were from the College of Chemistry in Jilin University (Changchun, China). Chemical inhibitors, ketoconazole (Ket), α-naphthoflavone (Naph), sulfaphenazole (Sul), quinidine (Qui), diethyl dithiocarbamate (DDC), ticlopidine hydrochloride (TP), and orphenadrine citrate salt (Orph) (purity >99%) were purchased from Sigma-Aldrich (Shanghai, China). Pooled human hepatic microsomes (20 mg/ml, liver sources were 10 male donors who died of trauma, ranging in age from 24 to 38 years) were purchased from the Research Institute for Liver Diseases Co. Ltd (Shanghai, China). cDNA-expressed human P450 isoforms (CYP3A4, CYP3A5, CYP1A2, CYP2C9*1, CYP2C19, CYP2D6*1, CYP2B6, CYP2E1, CYP1A1, and CYP1B2) from a baculovirus-infected cell system coexpressing human P450 reductase were purchased from BD Biosciences (San Jose, CA).The P450 content ranged from 1000 to 2000 pmol/ml. Glucose 6-phosphate (6-P-G) (purity 98–100%), $NADP^+$ (purity 97%), and glucose-6-phosphate dehydrogenase (PDH) (200–400 units/mg protein) were purchased from Sigma-Aldrich. 32 Digoxin (internal standard) was obtained from the National Institute for Control of Pharmaceutical and Biological Products (Beijing, China). High-performance liquid chromatography-grade acetonitrile and methanol were obtained from Merck (Darmstadt, Germany). Deionized water was purified using a Milli-Q system (Millipore Corporation, Billerica, MA). Magnesium chloride ($MgCl_2$), *n*-butanol, and other regents were all of analytical grade. Pooled human hepatic microsomes and human recombinant P450 isoforms were stored at −80°C until use.

Rat Hepatic Microsomes Preparation. All rats used in our experiments were male Sprague-Dawley rats (200–220 g b.wt.) from Academy of Military Medical Sciences (Beijing, China). All animal studies were approved by the Animal Ethics Committee of China Pharmaceutical University. Microsomes were prepared by using the livers of male rats through differential centrifugation (Hao et al., 2007; Jia and Liu, 2007). The protein concentrations were determined with a commercially available kit (BCA protein assay; Pierce Chemical, Rockford, IL). Rat hepatic microsomes were stored at −80°C and used within 2 weeks.

Metabolic Profiling of PPT Ginsenosides in Microsomal Incubation Systems. PPT ginsenosides were incubated in rat and human hepatic microsomes to examine the potential P450-mediated metabolism. For NADPH-dependent oxidative metabolism study, the reaction media contained microsomal protein (1 mg/ml for rat hepatic microsomes and 0.25 mg/ml for human hepatic microsomes), 10 mM 6-P-G, 10 mM $MgCl_2$, 1 U/ml PDH, 8 μM concentrations of each substrate (Re, Rg1, Rg2, Rf, Rh1, or PPT), and 0.5 mM $NADP^+$ in 100 mM potassium phosphate (pH 7.4). Negative control incubations containing no NADPH-regenerating system were conducted. All incubations were performed at 37°C in a shaking water bath for 30 min.

All samples were extracted by *n*-butanol and analyzed using LC/MS-IT-TOF (Shimadzu, Kyoto, Japan). A Shim-Pack VP-ODS C18 column (250 mm × 2.0 mm, 5 μm; Shimadzu) was used for chromatographic separation. The mobile phase consisted of water (A) and acetonitrile (B). The gradient program was set as follows: 20% B to 70% B from 0 to 20 min, 70% B to 20% B from 20 to 25 min, and then holding at 20% B for another 5 min. The flow rate was set at 0.2 ml/min with the column temperature at 35°C. Mass spectrometry was performed under negative ion scan mode with the scan range set at *m/z* 100 to 1200. The nebulizing gas flow rate was set at 1.5 l/min, and the drying gas pressure was 0.1 MPa. The applied voltage was −3.5 kV. The curved desolvation line temperature was 200°C.

Enzyme Kinetics in Rat and Human Hepatic Microsomes. Enzyme kinetics were determined in rat hepatic microsomes (1 mg/ml) and human hepatic microsomes (0.25 mg/ml) for four PPT ginsenosides [Rg2 (1.56–50 μM), Rf (2.5–80 μM), Rh1 (0.31–50 μM), and PPT (0.31–50 μM)] for which P450-catalyzed metabolism had been confirmed in the metabolic profiling study. Each assay tube contained the same NADPH-regenerating system described above. All reactions were conducted at 37°C for 15 min. Preliminary experiments were performed to ensure that the depletion of parent compounds was in the linear range of both reaction time and the protein concentration of microsomes.

Chemical Inhibition Study in Rat and Human Hepatic Microsomes. The chemical inhibition study was performed by adding each of the specific chemical inhibitors of P450 isoforms into the incubations of Rg2 (8 μM), Rf (8 μM), Rh1 (8 μM), and PPT (4 μM) in the rat and human microsomal incubation systems containing an NADPH-regenerating system as described above. The selective inhibitors and their concentrations were selected on the basis of previous reports and are as follows: Ket (1 μM) for CYP3A, Naph (10 μM) for CYP1A2, Sul (10 μM) for CYP2C, Qui (10 μM) for CYP2D, DDC (20 μM) for CYP2E1, TP (5 μM) for CYP2C19, and Orph (20 μM) for CYP2B (Rodrigues, 1999; Tucker et al., 2001; Bjornsson et al., 2003; Liu et al., 2007; Meyer et al., 2009). All reactions were initiated by addition of the substrates (ginsenosides). For the mechanism-based inhibitors, TP, DDC, and Orph were preincubated with all incubation constituents at 37°C for 15 min before the reaction was initiated by addition of substrates.

Metabolism of PPT Ginsenosides in Recombinant Human P450 Isoforms. The capacity of selected major human P450 isoforms to metabolize Rg2 (5 and 50 μM), Rf (5 and 50 μM), Rh1 (5 and 50 μM), and PPT (2 and 20 μM) was screened using human recombinant isozymes. In brief, each ginsenoside was added into a 0.2-ml incubation mixture containing P450 isoform (4 pmol for CYP3A4, CYP3A5, CYP1A2, and CYP2C9*1; 8 pmol for CYP2C19 and CYP2B6; 0.25 pmol for CYP1A1; 1 pmol for CYP1B1; 20 pmol for CYP2E1; and 2 pmol for CYP2D6*1), 1.3 mM $NADP^+$, 3.3 mM 6-P-G, 0.4 U/ml PDH, and 3.3 mM $MgCl_2$ in 100 mM potassium phosphate (pH 7.4). Reactions were initiated by adding substrate and incubated at 37°C

Downloaded from dmd.aspetjournals.org at Beijing Book Co Inc/PeriodicalsZhejiang Med Univ Lib/783081 on May 2, 2013

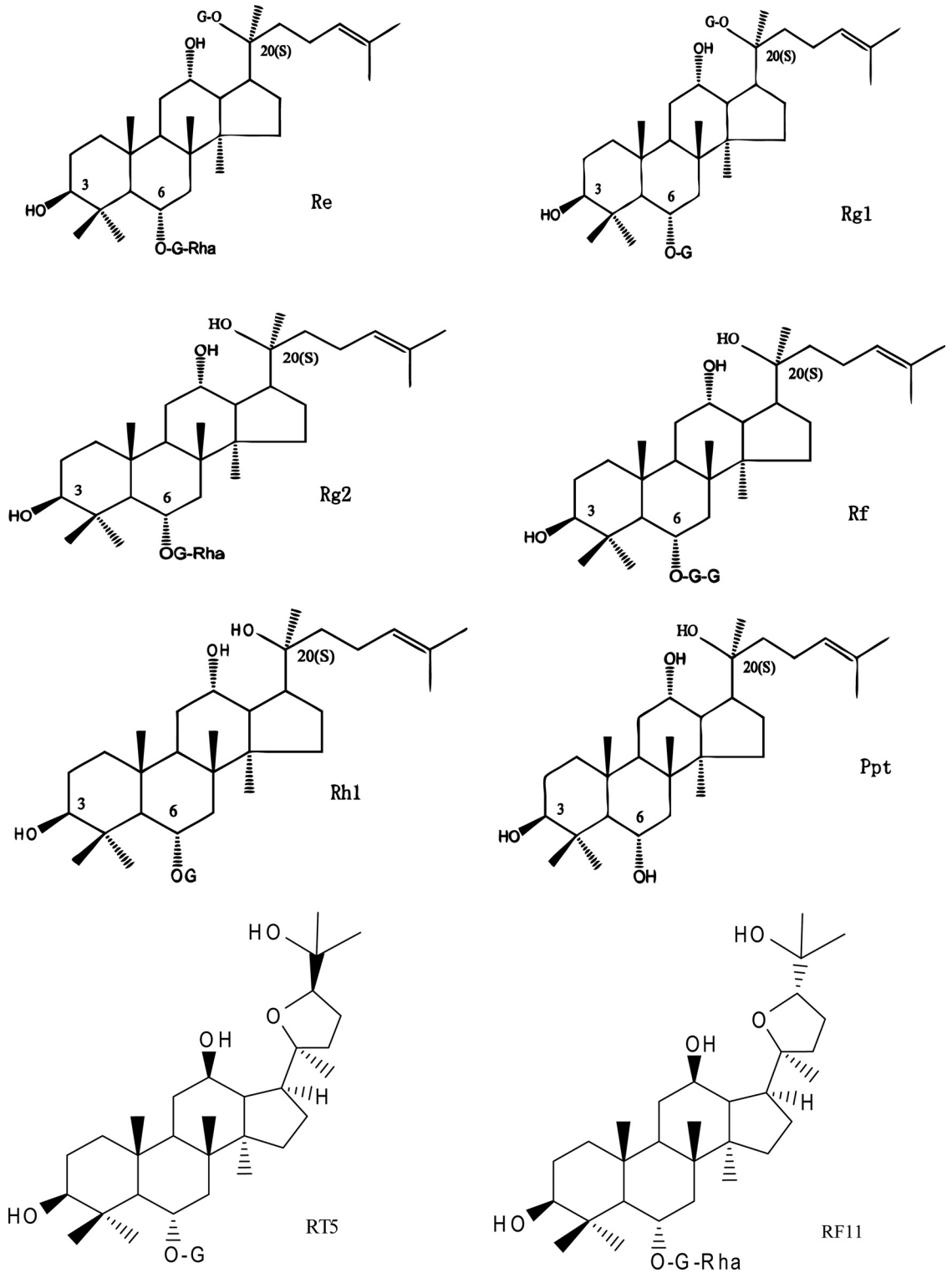

FIG. 1. Chemical structures of PPT-type ginsenosides, aglycone PPT, and pseudo-ginsenoside RF11 (metabolite for Rg2) and RT5 (metabolite for Rh1).

for 15 min. In a follow-up study to estimate kinetic parameters, Rg2 (1.56–50 μM), Rf (2.5–80 μM), Rh1 (0.31–50 μM), and PPT (0.31–50 μM) were incubated with human recombinant CYP3A4 (20 pmol/ml) for 15 min.

Quantitative Analysis. All reactions for quantitative analysis in rat and human hepatic microsomes and human recombinant P450 isoforms were terminated by addition of cold *n*-butanol with digoxin as their internal standard. The precipitate was removed by centrifugation, and the supernatant was transferred to an Eppendorf tube and evaporated to dryness by the Thermo Savant SPD 2010 SpeedVac System (Thermo Fisher Scientific, Waltham, MA). The residue was dissolved by mobile phase for analysis.

PPT ginsenosides and their aglycone PPT were quantified by a method based on our previous report (Sun et al., 2005) with slight modifications. All samples were analyzed by high-performance liquid chromatography/electrospray ionization/mass spectrometry (Shimadzu). Quantitative analysis was performed in selected ion monitoring mode. In brief, a Shim-Pack VP-ODS C18 column (250 mm × 2.0 mm, 5 μm) was used. The column

DMD DRUG METABOLISM AND DISPOSITION aspet
Downloaded from dmd.aspetjournals.org at Beijing Book Co Inc/PeriodicalsZhejiang Med Univ Lib/783081 on May 2, 2013

DMD DRUG METABOLISM AND DISPOSITION aspet

temperature was at 40°C. The nebulizing gas flow rate was set at 1.5 l/min, and the drying gas flow rate was 4.0 l/min. Mass spectrometry was performed under negative ion mode with the detector potential at 1.60 kV. The curved desolvation line temperature was 200°C. The mobile phase consisted of 2 mM ammonium chloride (A) and acetonitrile (B) with a gradient program as follows: 20% B to 60% B from 0 to 4.5 min, 60% B to 90% B from 4.5 to 6.5 min, 90% B to 20% B from 6.5 to 8.5 min, and holding at 20% B for another 4 min, with the flow rate set at 0.2 ml/min. The ($[M + Cl]^-$) ion, which has been found to be most sensitive for all analytes, was selected for the quantifications of Re at *m/z* 981.5, Rg1 at *m/z* 835.5, Rg2 at *m/z* 819.5, Rf at *m/z* 835.5, Rh1at *m/z* 673.5, PPT at *m/z* 511.5, and the internal standard digoxin at *m/z* 815.4.

Data Analysis. Kinetic parameters were analyzed using a method of parent drug depletion. Because oxygenation metabolism was the sole pathway for PPT ginsenosides in hepatic microsomes, the depletion rate of parent compounds may be indicative of the conglomeration rate of their oxygenation metabolism. The depletion profiles for all of the ginsenosides tested were preliminarily confirmed, exhibiting log-linear characteristics over the time course studied (15 min). The average depletion rate, expressed as picomoles per minute per milligram of protein, was then estimated from the differences between the zero time point and the time point after a 15-min incubation. The apparent V_{max} and K_m values were estimated by nonlinear regression from the Lineweaver-Burk plots based on the typical Michaelis-Menten equation, $1/V = 1/V_{max} + (K_m/V_{max}) \cdot 1/[S]$, where V is the rate of reaction, V_{max} is the maximum velocity, K_m is the Michaelis constant (substrate concentration at 0.5 V_{max}), and $[S]$ is the substrate concentration. The intrinsic clearance (CL_{int}) was calculated as V_{max}/K_m. Data are expressed as the mean ± S.D. of triplicate experiments.

Results

Metabolite Profiles. In both rat and human hepatic microsomal incubation systems, Rg2, Rh1, Rf, and PPT underwent efficient depletion, whereas the elimination of Re and Rg1 was negligible after a 30-min incubation. Samples from Rg2, Rh1, Rf, and PPT incubations were then subjected to a powerful LC/MS-IT-TOF analysis for metabolite profiling and identification. As a result, three metabolites for each of the PPT ginsenosides were detected. The chromatographic and mass data are summarized in Table 1. With accurate measurements of both parent and product ions, it was feasible to characterize the metabolites. For Rg2, Rf, and Rh1, three metabolites characterized with exactly the same quasi-molecular ions and different retention times were observed. The metabolites were readily proposed to be the monooxygenated products of the intact ginsenosides from an approximately 16-Da difference between the metabolites and their respective precursors. The major fragment patterns of such ginsenosides and M1/2 were of sequential sugar loss and further C20 aliphatic branch chain dissociation from the molecular ions to finally produce an aglycone PPT diagnostic ion at *m/z* 391. In contrast, fragment ions of M3 were somewhat different in that a diagnostic ion at *m/z* 415 instead of *m/z* 391 was observed. By a comparison with the respective authentic standards (Figs. 1 and 2; Table 1), M3 was identified as an ocotillol-type ginsenoside, and the oxygenation site was located on the C24–25 double bond. For M1/2, we could only propose an oxygenation site on the C20 aliphatic branch chain, considering that the typical aglycone ion characterized with *m/z* 391 was observed. For PPT, three monooxygenated metabolites (M1-1/2/3) and three dioxygenated metabolites (M2-1/2/3) were observed. As seen from the diagnostic ion at *m/z* 415, M1-1 and M2-1 were suggested to be the C24–25 double bond oxygenation metabolites.

Enzyme Kinetics in Rat and Human Hepatic Microsomes. If we consider that oxygenation was the predominant metabolic pathway of Rg2, Rf, Rh1, and PPT in the microsomal incubation system, the elimination rate of parent compound was quantified to represent the enzyme kinetics of the oxygenation metabolism of these four ginsenosides. The concentration of microsomal protein and the incubation time were optimized to ensure linear depletion of parent compounds. Kinetic plots shown in Figs. 3 and 4 indicate that the metabolic eliminations of these ginsenosides fit well to the Michaelis-Menten equation. Kinetic parameters including K_m, V_{max}, and CL_{int} are presented in Table 2. In human hepatic microsomes, the K_m value ranged from 16.8 (PPT) to 42.8 μM (Rf), and the V_{max} value ranged from 67.1 (Rg2) to 116.1 (PPT) pmol/min/mg protein. The intrinsic clearance (CL_{int}) calculated as V_{max}/K_m for the three PPT ginsenosides and their aglycone PPT ranked as follows: Rg2 ≤ Rf < Rh1 < PPT. Enzyme kinetic parameters determined from rat hepatic microsomes were comparable with those from human hepatic microsomes, except for slight differences between Rg2 and Rf.

Chemical Inhibition Study in Rat and Human Hepatic Microsomes. To phenotype the P450 isoforms involved in the oxygenation metabolism of PPT ginsenosides, various specific chemical inhibitors were used, and the substrate concentration was selected

TABLE 1

Summary of retention times, quasi-molecular ions, MS/MS product ions and predicted molecular formula for metabolites identification of PPT-type ginsenosides

Compounds	T_R	$[M - H]^-$	MS/MS Fragment Ions	Predicted Molecular Formula
	min			
Rg2	11.9	783.4893	637.4269, 619.4161, 475.3762, 457.3663, 391.2838	$C_{42}H_{72}O_{13}$
M1	7.2	799.4844	653.424, 635.4182, 491.3714, 391.2878	$C_{42}H_{72}O_{14}$
M2	8.4	799.4844	653.4249, 635.4108	$C_{42}H_{72}O_{14}$
M3 (RF11)[a]	10.9 (10.9)	799.4844 (799.4836)	653.4254 (653.4245), 635.4121 (635.4121), 491.3677 (491.3737), 415.3156 (415.3156)	$C_{42}H_{72}O_{14}$
Rf	10.9	799.4775	637.4201, 619.4103, 475.3714, 457,3578, 391.2792, 389.2688	$C_{42}H_{72}O_{14}$
M1	6.2	815.4762	653.4133, 491.3642, 391.2772	$C_{42}H_{72}O_{15}$
M2	7.4	815.4762	653.4157, 491.3661	$C_{42}H_{72}O_{15}$
M3	9.9	815.4762	653.4112, 491.3661	$C_{42}H_{72}O_{15}$
Rh1	12.3	637.4309	475.3795, 457.3684, 391.2869	$C_{36}H_{62}O_9$
M1	7.2	653.4262	491.3711, 391.2872	$C_{36}H_{62}O_{10}$
M2	8.5	653.4262	491.3761	$C_{36}H_{62}O_{10}$
M3 (RT5)	11.2 (11.2)	653.4262 (653.4275)	491.3767 (491.3754), 415.3156 (415.3156)	$C_{36}H_{62}O_{10}$
PPT	19.8	475.3719	457.3604, 391.2788, 373.2627	$C_{30}H_{52}O_4$
M1-1	12.7	491.3675	415.3138, 403.3146, 397.3026, 395.2917, 391.2771	$C_{30}H_{52}O_5$
M1-2	14.1	491.3675	473.3514, 455.3420, 391.2782, 373.2652, 371.2572	$C_{30}H_{52}O_5$
M1-3	15.6	491.3675	473.3578, 455.3514, 391.2779	$C_{30}H_{52}O_5$
M2-1	9.8	507.3616	489.3486, 471.3360, 431.3022, 429.3219, 391.2768	$C_{30}H_{52}O_6$
M2-2	10.3	507.3616	489.3484, 431.3055, 391.2784	$C_{30}H_{52}O_6$
M2-3	12.2	507.3616	431.3022, 403.3128	$C_{30}H_{52}O_6$

MS/MS, selected MS^2 scan in ion-trap; T_R, retention time.
[a] Data in parentheses were obtained from the study of authentic standards RF11 and RT5.

Downloaded from dmd.aspetjournals.org at Beijing Book Co Inc/PeriodicalsZhejiang Med Univ Lib/783081 on May 2, 2013

DMD DRUG METABOLISM AND DISPOSITION aspet

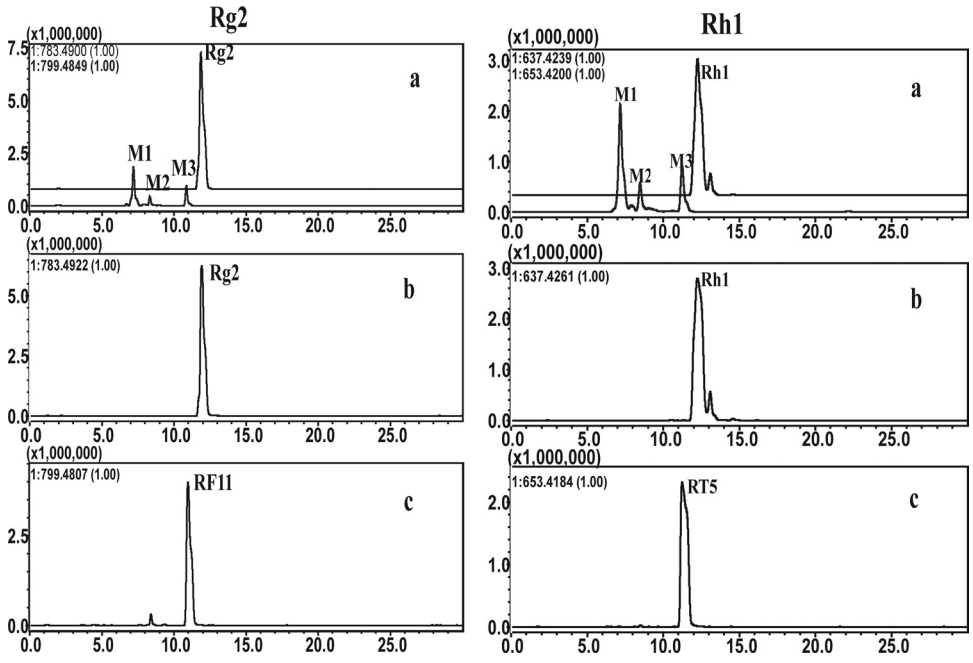

FIG. 2. Representative extracted ion chromatograms obtained from human microsomal incubation with Rg2 and Rh1. a, microsomal incubation samples. b and c, authentic compounds. In the metabolic profiling assay, ginsenosides (8 μM) were incubated in rat or human microsomes for 30 min. Samples were extracted by *n*-butanol and analyzed using LC/MS-IT-TOF.

on the basis of the estimated apparent K_m. Among the chemical inhibitors used in the human hepatic microsomes incubation system, only Ket, a specific CYP3A4/5 inhibitor showed a significant inhibitory effect on the oxygenation metabolism of all the four compounds. The turnover rate in the Ket preincubated system decreased to be 33, 30, 45, and 22% of the control for Rg2, Rf, Rh1, and PPT, respectively. All other P450 isoform-specific inhibitors resulted in a negligible effect on the oxygenation metabolism of PPT ginsenosides (Fig. 5). Similar results were obtained from the rat hepatic microsome study (Fig. 6).

Metabolism of PPT Ginsenosides in Human P450 Isoforms. In an initial screening procedure, 10 kinds of P450 isoforms were selected (Sauer et al., 2009) to determine the specific P450 isozymes involved in the oxygenation metabolism of the four PPT ginsenosides

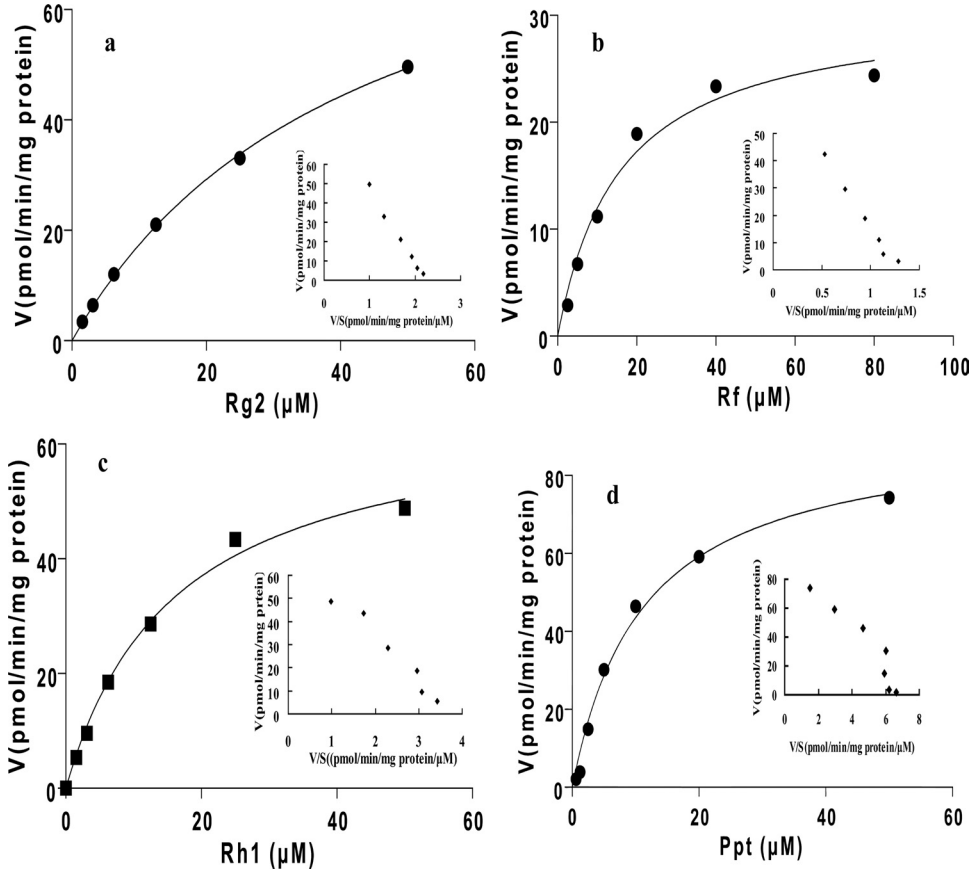

FIG. 3. Representative kinetic plots for the oxygenation metabolism of Rg2 (a), Rf (b), Rh1 (c), and PPT (d) in rat hepatic microsomes. Inset, Eadie-Hofstee plots. Ginsenoside Rg2 (1.56–50 μM), Rf (2.5–80 μM), Rh1 (0.31–50 μM), or PPT (0.31–50 μM) was incubated in rat hepatic microsomes (1.0 mg/ml) containing an NADPH-regenerating system for 15 min at 37°C. The average depletion rate (*y*-axis, picomoles per minute per milligram of protein) was estimated from the difference between the zero time point and the time point after a 15-min incubation. Plots provided are one representative of triplicate experiments, and the kinetic parameters obtained are summarized in Table 2.

Downloaded from dmd.aspetjournals.org at Beijing Book Co Inc/PeriodicalsZhejiang Med Univ Lib/783081 on May 2, 2013

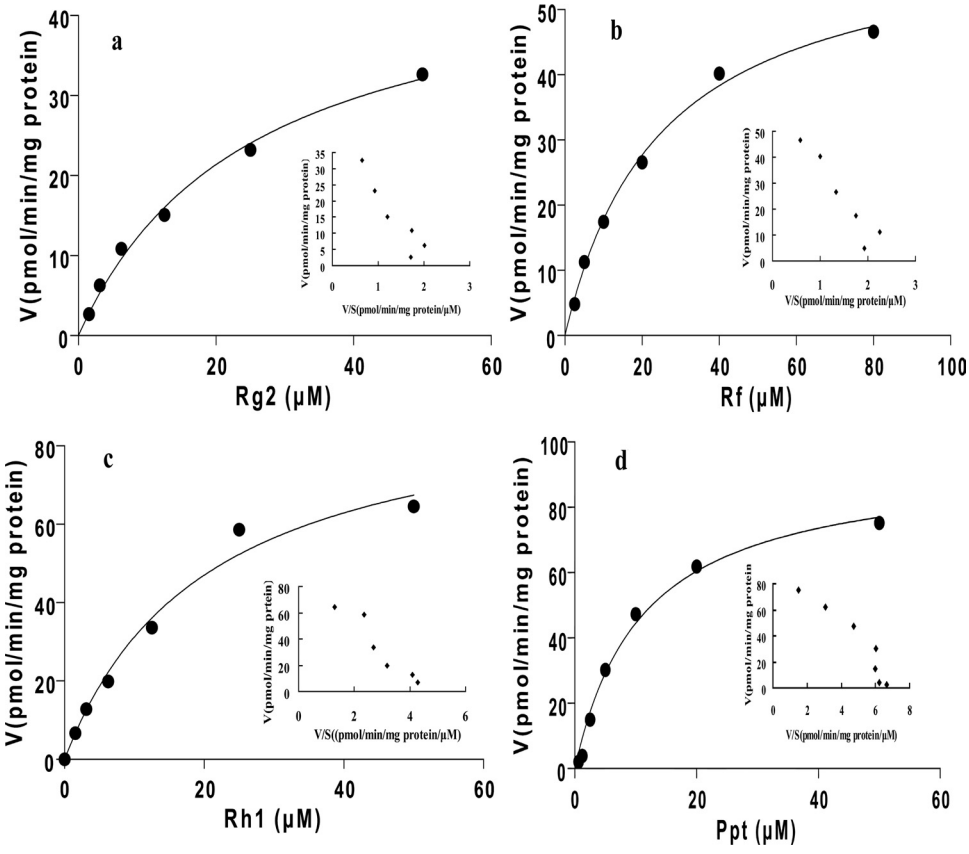

FIG. 4. Representative kinetic plots for the oxygenation metabolism of Rg2 (a), Rf (b), Rh1 (c), and PPT (d) in human hepatic microsomes. Inset, Eadie-Hofstee plots. Ginsenoside Rg2 (1.56–50 μM), Rf (2.5–80 μM), Rh1 (0.31–50 μM), or PPT (0.31–50 μM) was incubated in human hepatic microsomes (0.2 mg/ml) containing an NADPH-regenerating system for 15 min at 37°C. The average depletion rate (*y*-axis, picomoles per minute per milligram of protein) was estimated from the difference between the zero time point and the time point after a 15-min incubation. Plots provided are one representative of triplicate experiments, and the kinetic parameters obtained are summarized in Table 2.

Rg2, Rf, Rh1, and PPT at two substrate concentrations. Among the 10 P450s tested, only CYP3A4 and, to a very minor extent, CYP3A5 exerted catalytic activity toward the oxygenation metabolism of all the compounds tested, whereas the metabolic elimination of parent compounds was negligible in the incubations with the other 8 isoforms. As shown in Table 3, the PPT ginsenoside turnover rate in the CYP3A4 incubation was much higher (ranged from 12- to 48-fold) than that in the CYP3A5 incubation.

Therefore, we conducted a follow-up enzyme kinetic study of these ginsenosides in the recombinant CYP3A4 isoform only. As observed in both the human and rat hepatic liver microsome study, PPT showed the highest V_{max} value at 92.6 pmol/(min · pmol) protein. The K_m values of PPT and Rh1 were comparable and much lower than those for Rg2 and Rf. The intrinsic clearance (V_{max}/K_m) ranked as follows: Rf ≤ Rg2 < Rh1 < PPT, which was generally consistent with that determined from both the human and rat hepatic microsome studies (Table 2).

Discussion

The class of PPT-type ginsenosides is one of the important classes of ginsenosides in addition to the PPD-type ginsenosides. Their powerful and wide-ranging pharmacological activities and their potential to serve as drug leads have attracted much attention from researchers worldwide. PPT ginsenosides have recently been found to be effective in modulating the central nervous (Wang et al., 2009), immunological (Sun et al., 2006, 2007), cardiovascular (Li and Liu, 2008), and metabolic systems (Chang et al., 2007) and in cancer treatment (Wang and Yuan, 2008). In view of these pharmacological merits of PPT ginsenosides, it is thus very important to explore their biological transformation and metabolic pathways for better understanding of their systematic disposition and benefits. Previous reports focused mainly on the presystematic degradation of PPT ginsenosides in the gastrointestinal tract, whereas very little is known about hepatic

TABLE 2

Enzyme kinetic parameters for PPT-type ginsenosides metabolism by rat, human hepatic microsomes, and human recombinant CYP3A4 isoform

Kinetic parameters were estimated from the Michaelis-Menten equation by nonlinear regression analysis of the depletion rate of parent compounds versus substrate concentration data. Data provided are the means ± S.D. of triplicate experiments for microsomes and the mean of duplicate experiments for recombinant enzymes.

Parameters	PPT	Rh1	Rg2	Rf
Rat hepatic microsomes				
V_{max} [pmol/(min · mg) protein]	118.2 ± 8.9	82.1 ± 7.5	83.9 ± 4.3	61.7 ± 2.2
K_m (μM)	17.5 ± 0.6	19.3 ± 1.0	35.4 ± 1.8	46.0 ± 1.2
V_{max}/K_m ratio [μl/(min · mg) protein]	6.8 ± 0.7	4.3 ± 0.5	2.4 ± 0.2	1.3 ± 0.1
Human hepatic microsomes				
V_{max} [pmol/(min · mg) protein]	116.1 ± 6.5	85.1 ± 2.3	67.1 ± 4.5	87.9 ± 9.5
K_m (μM)	16.8 ± 1.4	17.9 ± 1.0	34.8 ± 2.9	42.8 ± 4.5
V_{max}/K_m ratio [μl/(min · mg) protein]	6.9 ± 0.3	4.8 ± 0.2	1.9 ± 0.1	2.1 ± 0.1
CYP3A4 isoform				
V_{max} [pmol/(min · mg) protein]	92.6	59.2	62.1	59.5
K_m (μM)	15.0	14.2	30.2	44.6
V_{max}/K_m ratio [μl/(min · mg) protein]	6.2	4.2	2.1	1.3

DRUG METABOLISM AND DISPOSITION DMD aspet
Downloaded from dmd.aspetjournals.org at Beijing Book Co Inc/PeriodicalsZhejiang Med Univ Lib/783081 on May 2, 2013

DMD DRUG METABOLISM AND DISPOSITION aspet

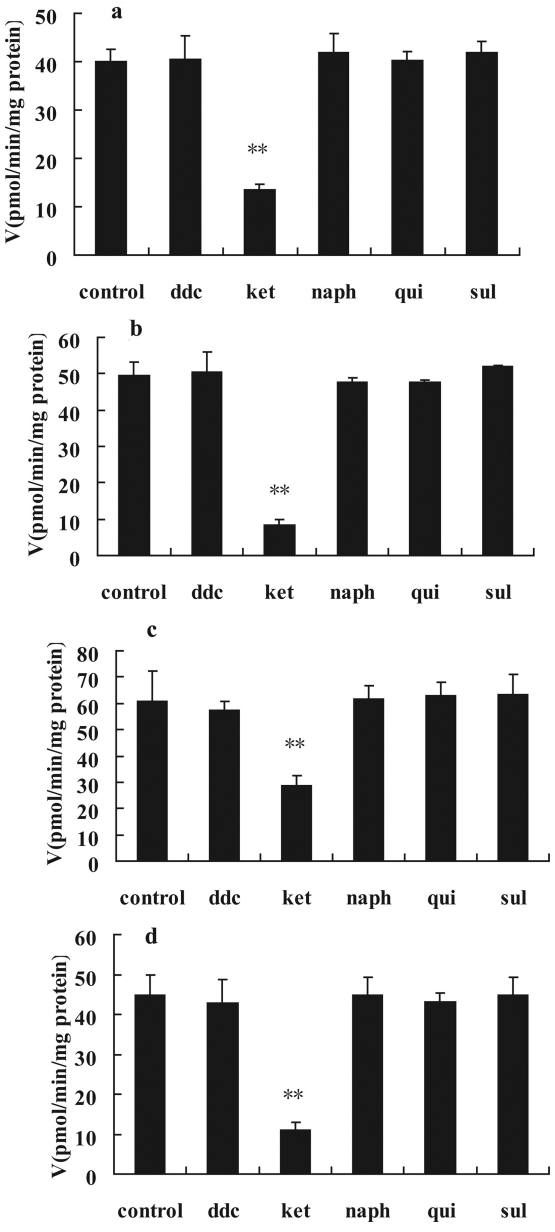

FIG. 5. Effects of chemical inhibitors on the oxygenation metabolism of Rg2 (a), Rf (b), Rh1 (c), and PPT (d) in rat hepatic microsomes. The substrate concentration selected was 8 μM for Rg2, Rf, and Rh1 and 4 μM for Ppt.

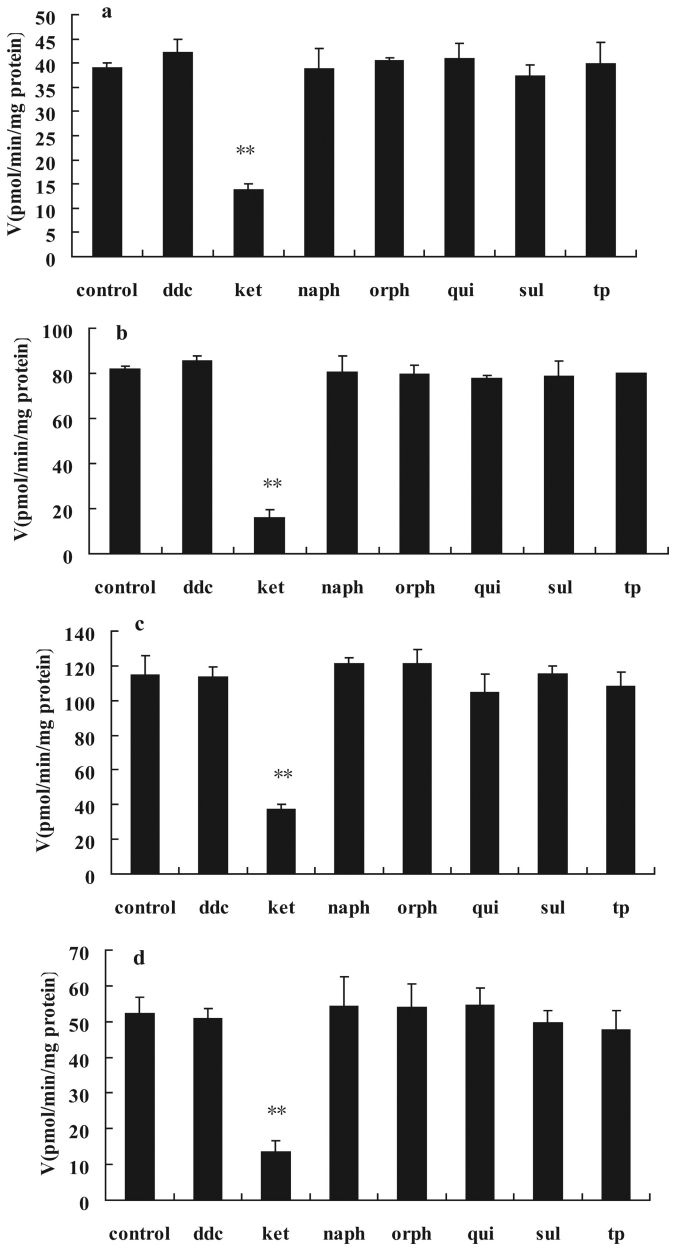

FIG. 6. Effects of chemical inhibitors on the oxygenation metabolism of Rg2 (a), Rf (b), Rh1 (c), and PPT (d) in human hepatic microsomes. The substrate concentration selected was 8 μM for Rg2, Rf, and Rh1 and 4 μM for Ppt.

microsomal-mediated metabolism. Although oral bioavailability and plasma levels of ginsenosides are generally low because of their extensive presystematic metabolism and poor membrane permeability (Tawab et al., 2003), previous studies from our laboratory and others showed that the hepatic levels of ginsenosides after oral ingestion were much higher than those in plasma and other tissues (Gu et al., 2009; Liu et al., 2009). In addition, oxygenated metabolites have actually been identified in bile and urine samples after oral ingestion of ginsenosides (Lai et al., 2009a; Liu et al., 2009). Such evidence suggests that hepatic cytochrome P450 may play an important role in the systematic disposition of ginsenosides. In the present study, five major PPT-type ginsenosides including Re, Rg1, Rg2, Rf, and Rh1 and the aglycone PPT were selected to explore the general principles of cytochrome P450-catalyzed metabolism of PPT-type ginsenosides.

NADPH-dependent P450-catalyzed oxygenation metabolism of PPT ginsenosides was confirmed in this study in both rat and human hepatic microsomal incubation systems. On the basis of a powerful LC/MS-IT-TOF analysis that had been well developed in our laboratory for identification of multiple compounds from a complex matrix

TABLE 3

Metabolic rates of ginsenosides by human recombinant CYP450 isoforms

CYP450 Isoforms[a]	Metabolic Rate							
	PPT		Rh1		Rg2		Rf	
	2 μM	20 μM	5 μM	50 μM	5 μM	50 μM	5 μM	50 μM
	pmol/(min · pmol) protein							
3A4	3.99	33.77	6.36	27.91	4.68	25.39	3.01	23.99
3A5	0.19	0.71	0.19	0.71	0.3	2.02	0.18	1.01

[a] A panel of 10 recombinant human P450 isoforms was screened, and only CYP3A4 and, to a very minor extent, CYP3A5 were found to be active toward the oxygenation metabolism of PPT-type ginsenosides.

Downloaded from dmd.aspetjournals.org at Beijing Book Co Inc/PeriodicalsZhejiang Med Univ Lib/783081 on May 2, 2013

DMD DRUG METABOLISM AND DISPOSITION aspet

(Hao et al., 2008a; Zheng et al., 2009), three monooxygenated metabolites for each of the PPT ginsenosides and three monooxygenated and three double-oxygenated metabolites for the aglycone PPT were identified from the microsomal incubation media. As seen from the fragment patterns of both parent compounds and metabolites, the oxygenation metabolism site on the C20 aliphatic branch chain was proposed. This result obtained from the in vitro hepatic microsome incubations was consistent with our previous study in vivo of Rh1 (Lai et al., 2009a) and also with previous reports in vivo of the typical PPD ginsenosides Rh2 (Qian et al., 2005a) and Rb1 (Qian et al., 2006). By a comparison with the authentic standards (RF11 and RT5), one of the oxygenation sites was confirmed on the C24–25 double bond to produce C20–24 epoxides (ocotillol-type ginsenosides) after rearrangement immediately from the C24 and C25 epoxides.

As seen from this study and the previous reports for both PPD and PPT ginsenosides, microsomal P450-catalyzed oxygenation metabolism plays an important role in the systematic elimination of ginsenosides. Thus, it should be of great interest to determine the specific P450 isoforms involved in the oxygenation metabolism for better understanding of the pharmacokinetics and disposition of ginsenosides in different species and previously reported ginseng-drug interactions. For this purpose, the specific P450 isoforms responsible for the oxygenation metabolism of PPT ginsenosides were determined on the basis of a chemical inhibition study and recombinant P450 isoform screening. All evidence obtained in the present study supported CYP3A being the sole isoform involved in the oxygenation metabolism of ginsenosides. It has been well known that CYP3A is the most abundant human hepatic P450 isoforms and accounts for the metabolism of approximately 50% of known drugs. CYP3A4 and CYP3A5 are the two major isoforms in the CYP3A family in human adults and share 84% sequence homology and many substrates overlapping. In this study, it has been found that the typical PPT ginsenoside turnover rate in CYP3A4 was much higher (ranging from 12- to 48-fold) than that in CYP3A5, suggesting that CYP3A4 should be the predominant isoform and that CYP3A5 contributed very little to the oxygenation metabolism of ginsenosides. Such a phenomenon has been also widely found for many other typical CYP3A substrates such as buspirone (Zhu et al., 2005) and cyclosporin A.

To explore the structure-metabolism relationship of PPT ginsenosides, the detailed enzyme kinetics of four major ginsenosides were performed in rat and human microsomal and also in recombinant CYP3A4 incubation systems. Among the components tested in this study, Re and Rg1 structurally characterized with a glucose substitution at the C20 hydroxy group underwent negligible metabolism, whereas the other four compounds without glucose substitution at the C20 hydroxy group exhibited efficient metabolic elimination in the microsomal incubation systems. The experimental determined intrinsic clearance for Rg2, Rf, Rh1, and PPT was generally consistent throughout rat and human microsomal and human recombinant CYP3A4 incubation systems and ranked as Rf $\leq$ Rg2 $<$ Rh1 $<$ PPT. Considering that the active site of CYP3A4 had been claimed to be hydrophobic (Williams et al., 2004; Yano et al., 2004), we sought to discover whether the intrinsic clearances of PPT ginsenosides by CYP3A4 were correlated with their hydrophobicity. The typical hydrophobic parameter logP values for Rf, Rg2, Rh1, and PPT were 2.7, 3.2, 4.3, and 5.9, respectively, which was found to be correlated well with their intrinsic clearance in the human recombinant CYP3A4 isozyme ($r^2 = 0.99$). The logP value may be a useful descriptor for at least qualitatively predicting the metabolic stability of ginsenosides by CYP3A4, as that proposed for other CYP3A4 substrates (Marechal et al., 2006). Results obtained from this study clearly reveal a general structure-metabolism relationship for the CYP3A4-catalyzed oxygenation metabolism of PPT ginsenosides: the more glycosyl substitutions on the aglycone skeleton (the lower hydrophobicity), the lower binding affinity and intrinsic clearance by CYP3A4. The glycosyl substitution at the C20 hydroxy group seems to completely prevent metabolism of ginsenosides, whereas glycosyl substitution on the aglycone skeleton is likely to increase their metabolic resistance by CYP3A4. The same was true for the structure-activity relationship for inhibition of ginsenosides on CYP3A (Hao et al., 2008b). Such results strongly suggest that the previously reported CYP3A inhibitory effect of ginsenosides is in the mode of substrate-competitive.

In summary, the novel data obtained from this study strongly indicate that CYP3A4-catalyzed oxygenation metabolism plays an important role in the systematic clearance of PPT-type ginsenosides (Fig. 7). The glycosyl substitutions on the aglycone skeleton and especially at the C20 hydroxy group are likely to constitute steric hindrances to prevent the binding of ginsenosides to the active site of CYP3A4 and thus cause metabolic resistance. PPT and Rh1, characterized with K_m values at 15.0 and 14.2 μM, respectively, can possibly serve as new probe substrates for CYP3A4 in vitro, considering that CYP3A4 has been found to be the predominant, if not the sole, P450 isoform involved in microsomal-mediated metabolism. Findings from this study also provide novel explanations for the previously reported ginseng-drug interactions (Coon and Ernst, 2002; Bressler, 2005) and for the reason that only PPT and Rh1 but not their precursors exhibit competitive inhibition on CYP3A4 activity (Liu et al., 2004, 2006a,b; Etheridge et al., 2007; Hao et al., 2008b). However, it should be noted that although Re and Rg1 are not direct substrates of CYP3A4, they can be transformed to the CYP3A4 substrates Rh1 and PPT by gastric acid and intestinal bacteria and thus may also exert competitive inhibition of other CYP3A4 substrates. In addition, the present identification of PPT ginsenosides as CYP3A4 substrates provides novel insight into the understanding of the metabolism-based synergistic mechanism of herbal compound prescriptions (Sheng-Mai-San) (Xu et al., 2008) because we have previously found that the adjunct herb *Schisandra* is a strong modulator of CYP3A4 (Lai et al., 2009b).

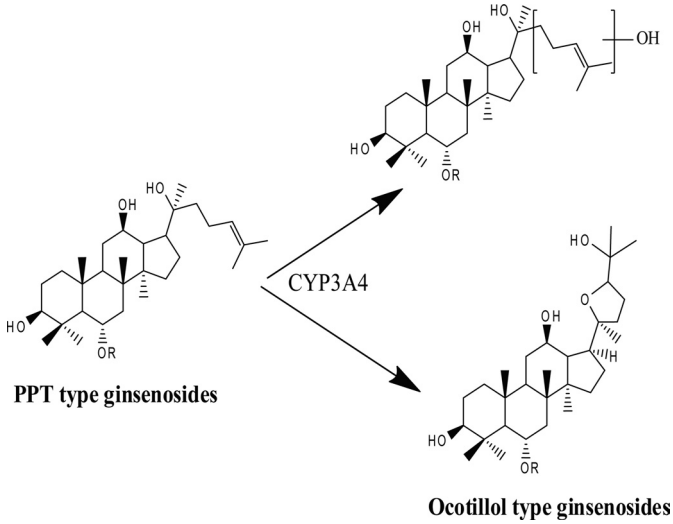

FIG. 7. CYP3A4-mediated oxygenation metabolism pathway of PPT-type ginsenosides. The oxygenation metabolism sites were confirmed on the C20 aliphatic branch chain, and the C24–25 double bond was identified as one of the major oxygenation sites, on the basis of the LC/MS-IT-TOF analysis and the use of authentic standards.

Downloaded from dmd.aspetjournals.org at Beijing Book Co Inc/PeriodicalsZhejiang Med Univ Lib/783081 on May 2, 2013

DMD
DRUG METABOLISM AND DISPOSITION
aspet

References

Attele AS, Wu JA, and Yuan CS (1999) Ginseng pharmacology: multiple constituents and multiple actions. *Biochem Pharmacol* **58:**1685–1693.

Bae EA, Han MJ, Kim EJ, and Kim DH (2004) Transformation of ginseng saponins to ginsenoside Rh2 by acids and human intestinal bacteria and biological activities of their transformants. *Arch Pharm Res* **27:**61–67.

Bjornsson TD, Callaghan JT, Einolf HJ, Fischer V, Gan L, Grimm S, Kao J, King SP, Miwa G, Ni L, et al. (2003) The conduct of in vitro and in vivo drug-drug interaction studies: a Pharmaceutical Research and Manufacturers of America (PhRMA) perspective. *Drug Metab Dispos* **31:**815–832.

Bressler R (2005) Herb-drug interactions: interactions between ginseng and prescription medications. *Geriatrics* **60:**16–17.

Chang TC, Huang SF, Yang TC, Chan FN, Lin HC, and Chang WL (2007) Effect of ginsenosides on glucose uptake in human Caco-2 cells is mediated through altered Na^+/glucose cotransporter 1 expression. *J Agric Food Chem* **55:**1993–1998.

Christensen LP (2009) Ginsenosides chemistry, biosynthesis, analysis, and potential health effects. *Adv Food Nutr Res* **55:**1–99.

Coon JT and Ernst E (2002) Panax ginseng: a systematic review of adverse effects and drug interactions. *Drug Saf* **25:**323–344.

Etheridge AS, Black SR, Patel PR, So J, and Mathews JM (2007) An *in vitro* evaluation of cytochrome P450 inhibition and P-glycoprotein interaction with goldenseal, *Ginkgo biloba*, grape seed, milk thistle, and ginseng extracts and their constituents. *Planta Med* **73:**731–741.

Gillis CN (1997) Panax ginseng pharmacology: a nitric oxide link? *Biochem Pharmacol* **54:**1–8.

Gu Y, Wang GJ, Sun JG, Jia YW, Wang W, Xu MJ, Lv T, Zheng YT, and Sai Y (2009) Pharmacokinetic characterization of ginsenoside Rh2, an anticancer nutrient from ginseng, in rats and dogs. *Food Chem Toxicol* **47:**2257–2268.

Hao H, Cui N, Wang G, Xiang B, Liang Y, Xu X, Zhang H, Yang J, Zheng C, Wu L, et al. (2008a) Global detection and identification of nontarget components from herbal preparations by liquid chromatography hybrid ion trap time-of-flight mass spectrometry and a strategy. *Anal Chem* **80:**8187–8194.

Hao H, Wang G, Cui N, Li J, Xie L, and Ding Z (2007) Identification of a novel intestinal first pass metabolic pathway: NQO1 mediated quinone reduction and subsequent glucuronidation. *Curr Drug Metab* **8:**137–149.

Hao M, Zhao Y, Chen P, Huang H, Liu H, Jiang H, Zhang R, and Wang H (2008b) Structure-activity relationship and substrate-dependent phenomena in effects of ginsenosides on activities of drug-metabolizing P450 enzymes. *PLoS One* **3:**e2697.

Jia L and Liu X (2007) The conduct of drug metabolism studies considered good practice (II): in vitro experiments. *Curr Drug Metab* **8:**822–829.

Jia L and Zhao Y (2009) Current evaluation of the millennium phytomedicine—ginseng (I): etymology, pharmacognosy, phytochemistry, market and regulations. *Curr Med Chem* **16:**2475–2484.

Jia L, Zhao Y, and Liang XJ (2009) Current evaluation of the millennium phytomedicine—ginseng (II): collected chemical entities, modern pharmacology, and clinical applications emanated from traditional Chinese medicine. *Curr Med Chem* **16:**2924–2942.

Kasai R, Hara K, Dokan R, Suzuki N, Mizutare T, Yoshihara S, and Yamasaki K (2000) Major metabolites of ginseng sapogenins formed by rat liver microsomes. *Chem Pharm Bull (Tokyo)* **48:**1226–1227.

Lai L, Hao H, Liu Y, Zheng C, Wang Q, Wang G, and Chen X (2009a) Characterization of pharmacokinetic profiles and metabolic pathways of 20(*S*)-ginsenoside Rh1 in vivo and in vitro. *Planta Med* **75:**797–802.

Lai L, Hao H, Wang Q, Zheng C, Zhou F, Liu Y, Wang Y, Yu G, Kang A, Peng Y, et al. (2009b) Effects of short-term and long-term pretreatment of *Schisandra lignans* on regulating hepatic and intestinal CYP3A in rats. *Drug Metab Dispos* **37:**2399–2407.

Li GX and Liu ZQ (2008) The protective effects of ginsenosides on human erythrocytes against hemin-induced hemolysis. *Food Chem Toxicol* **46:**886–892.

Liu H, Yang J, Du F, Gao X, Ma X, Huang Y, Xu F, Niu W, Wang F, Mao Y, et al. (2009) Absorption and disposition of ginsenosides after oral administration of *Panax notoginseng* extract to rats. *Drug Metab Dispos* **37:**2290–2298.

Liu Y, Li W, Li P, Deng MC, Yang SL, and Yang L (2004) The inhibitory effect of intestinal bacterial metabolite of ginsenosides on CYP3A activity. *Biol Pharm Bull* **27:**1555–1560.

Liu Y, Ma H, Zhang JW, Deng MC, and Yang L (2006a) Influence of ginsenoside Rh1 and F1 on human cytochrome p450 enzymes. *Planta Med* **72:**126–131.

Liu Y, Zhang JW, Li W, Ma H, Sun J, Deng MC, and Yang L (2006b) Ginsenoside metabolites, rather than naturally occurring ginsenosides, lead to inhibition of human cytochrome P450 enzymes. *Toxicol Sci* **91:**356–364.

Liu YT, Hao HP, Liu CX, Wang GJ, and Xie HG (2007) Drugs as CYP3A probes, inducers, and inhibitors. *Drug Metab Rev* **39:**699–721.

Marechal JD, Yu J, Brown S, Kapelioukh I, Rankin EM, Wolf CR, Roberts GC, Paine MJ, and Sutcliffe MJ (2006) In silico and in vitro screening for inhibition of cytochrome P450 CYP3A4 by comedications commonly used by patients with cancer. *Drug Metab Dispos* **34:**534–538.

Meyer MR, Peters FT, and Maurer HH (2009) Stereoselective differences in the cytochrome P450-dependent dealkylation and demethylenation of *N*-methyl-benzodioxolyl-butanamine (MBDB, Eden) enantiomers. *Biochem Pharmacol* **77:**1725–1734.

Qian T, Cai Z, Wong RN, and Jiang ZH (2005a) Liquid chromatography/mass spectrometric analysis of rat samples for in vivo metabolism and pharmacokinetic studies of ginsenoside Rh2. *Rapid Commun Mass Spectrom* **19:**3549–3554.

Qian T, Cai Z, Wong RN, Mak NK, and Jiang ZH (2005b) In vivo rat metabolism and pharmacokinetic studies of ginsenoside Rg3. *J Chromatogr B Analyt Technol Biomed Life Sci* **816:**223–232.

Qian T, Jiang ZH, and Cai Z (2006) High-performance liquid chromatography coupled with tandem mass spectrometry applied for metabolic study of ginsenoside Rb1 on rat. *Anal Biochem* **352:**87–96.

Rodrigues AD (1999) Integrated cytochrome P450 reaction phenotyping: attempting to bridge the gap between cDNA-expressed cytochromes P450 and native human liver microsomes. *Biochem Pharmacol* **57:**465–480.

Sauer C, Peters FT, Schwaninger AE, Meyer MR, and Maurer HH (2009) Investigations on the cytochrome P450 (CYP) isoenzymes involved in the metabolism of the designer drugs *N*-(1-phenyl cyclohexyl)-2-ethoxyethanamine and *N*-(1-phenylcyclohexyl)-2-methoxyethanamine. *Biochem Pharmacol* **77:**444–450.

Sun HX, Chen Y, and Ye Y (2006) Ginsenoside Re and notoginsenoside R1: immunologic adjuvants with low haemolytic effect. *Chem Biodivers* **3:**718–726.

Sun J, Hu S, and Song X (2007) Adjuvant effects of protopanaxadiol and protopanaxatriol saponins from ginseng roots on the immune responses to ovalbumin in mice. *Vaccine* **25:**1114–1120.

Sun J, Wang G, Haitang X, Hao L, Guoyu P, and Tucker I (2005) Simultaneous rapid quantification of ginsenoside Rg1 and its secondary glycoside Rh1 and aglycone protopanaxatriol in rat plasma by liquid chromatography-mass spectrometry after solid-phase extraction. *J Pharm Biomed Anal* **38:**126–132.

Tawab MA, Bahr U, Karas M, Wurglics M, and Schubert-Zsilavecz M (2003) Degradation of ginsenosides in humans after oral administration. *Drug Metab Dispos* **31:**1065–1071.

Tucker GT, Houston JB, and Huang SM (2001) Optimizing drug development: strategies to assess drug metabolism/transporter interaction potential—toward a consensus. *Pharm Res* **18:**1071–1080.

Wang CZ and Yuan CS (2008) Potential role of ginseng in the treatment of colorectal cancer. *Am J Chin Med* **36:**1019–1028.

Wang Y, Ye X, Ma Z, Liang Q, Lu B, Tan H, Xiao C, Zhang B, and Gao Y (2008) Induction of cytochrome P450 1A1 expression by ginsenoside Rg1 and Rb1 in HepG2 cells. *Eur J Pharmacol* **601:**73–78.

Wang YZ, Chen J, Chu SF, Wang YS, Wang XY, Chen NH, and Zhang JT (2009) Improvement of memory in mice and increase of hippocampal excitability in rats by ginsenoside Rg1's metabolites ginsenoside Rh1 and protopanaxatriol. *J Pharmacol Sci* **109:**504–510.

Williams PA, Cosme J, Vinkovic DM, Ward A, Angove HC, Day PJ, Vonrhein C, Tickle IJ, and Jhoti H (2004) Crystal structures of human cytochrome P450 3A4 bound to metyrapone and progesterone. *Science* **305:**683–686.

Xie HT, Wang GJ, Sun JG, Tucker I, Zhao XC, Xie YY, Li H, Jiang XL, Wang R, Xu MJ, et al. (2005) High performance liquid chromatographic-mass spectrometric determination of ginsenoside Rg3 and its metabolites in rat plasma using solid-phase extraction for pharmacokinetic studies. *J Chromatogr B Analyt Technol Biomed Life Sci* **818:**167–173.

Xu M, Wang G, Xie H, Huang Q, Wang W, and Jia Y (2008) Pharmacokinetic comparisons of schizandrin after oral administration of schizandrin monomer, *Fructus Schisandrae* aqueous extract and Sheng-Mai-San to rats. *J Ethnopharmacol* **115:**483–488.

Yang L, Deng Y, Xu S, and Zeng X (2007) In vivo pharmacokinetic and metabolism studies of ginsenoside Rd. *J Chromatogr B Analyt Technol Biomed Life Sci* **854:**77–84.

Yano JK, Wester MR, Schoch GA, Griffin KJ, Stout CD, and Johnson EF (2004) The structure of human microsomal cytochrome P450 3A4 determined by X-ray crystallography to 2.05-Å resolution. *J Biol Chem* **279:**38091–38094.

Zheng C, Hao H, Wang X, Wu X, Wang G, Sang G, Liang Y, Xie L, Xia C, and Yao X (2009) Diagnostic fragment-ion-based extension strategy for rapid screening and identification of serial components of homologous families contained in traditional Chinese medicine prescription using high-resolution LC-ESI- IT-TOF/MS: Shengmai injection as an example. *J Mass Spectrom* **44:**230–244.

Zhu M, Zhao W, Jimenez H, Zhang D, Yeola S, Dai R, Vachharajani N, and Mitroka J (2005) Cytochrome P450 3A-mediated metabolism of buspirone in human liver microsomes. *Drug Metab Dispos* **33:**500–507.

Address correspondence to: Dr. Guangji Wang, Key Laboratory of Drug Metabolism and Pharmacokinetics, China Pharmaceutical University, 24 Tong Jia Xiang, Nanjing 210009, China. E-mail: guangjiwang@hotmail.com

Downloaded from dmd.aspetjournals.org at Beijing Book Co Inc/PeriodicalsZhejiang Med Univ Lib/783081 on May 2, 2013